

The photocathode area of the Hamamatsu R1408 photomultiplier - SNO-STR-91-063

R. J. Boardman
Nuclear Physics Laboratory,
Keble Road,
Oxford OX1 3RH
England, UK

October 1991

The aim of the work described in this report is to determine the relative photon counting efficiency, as a function of position on the photocathode, of the SNO photomultipliers. The manufacture of the reflectors for the photomultipliers requires knowledge of the relative sensitivity of the photocathode (including photoelectron collection efficiency) as a function of the position of impact of an incident photon, particularly in the region near the boundary of the photocathode. The latter is required so that the diameter of the smaller aperture of the reflector can be determined. The latter should be made as large as possible in order to maximize the Čerenkov radiation collection from neutrino interactions. However, if the reflector covers an area larger than that of the photocathode, the optics of the reflector are compromised, and the efficiency of recording photons which originated at the centre of the detector is reduced.

The Hamamatsu R1408 photomultipliers used here are those made using the Schott 8246 low background glass, and are identical to those to be installed in the SNO detector. The photocathode diameter is nominally 200 mm. The photomultipliers were measured using identical bases and operating points as those to be used in the detector. The 5 photomultipliers used in this study was taken at random from a sample of 20 (SNO) Hamamatsu R1408 photomultipliers, and the Queens University spot scan apparatus was used to measure the relative efficiency as a function of position on the photocathode. In addition to the scan data, systematic checks were made to measure the positional accuracy and resolution of the apparatus. These parameters were found to be consistent with the expected values.

For brevity, only a brief summary of the Queens photocathode spot scan apparatus is given below. A source of Čerenkov radiation (^{90}Sr in acrylic) was used to provide illumination, which was collimated to a beam with a divergence of about 15° (full width half maximum). The exit aperture of the source had a length of about 10 mm and a slit width of about 2 mm, and the source was always used to scan the photomultiplier in a direction normal to the long axis of the slit. Hence the 2 mm width represents the smallest resolution possible with this apparatus. This source is rotated on a circle of radius 126 mm, and its position is monitored with an external pointer to indicate the angle of the source with respect to the axis of the photomultiplier. The direction of the scan with respect to the vein of the first dynode was chosen at random for the photomultipliers tested in this study¹.

¹This approach was used as the data were to be applied to the reflector design which requires some 'average'

Using the Hamamatsu R1408 photomultiplier, this geometry ensures that the source traverses the surface of the photomultiplier front window for angles smaller than the critical angle θ_c (about 40°). For angles larger than this the source moves off the surface of the photomultiplier by a short distance, thus degrading the resolution. The R1408 photomultiplier under test was aligned between four posts, which center the PMT about the 0° position of the source. The PMT is mounted so that the source just touches the PM in the 0° position. This alignment is thought to be accurate at the level 1 mm, and this was latter confirmed by the deduced position of a test mask, see below. Also the observation of symmetry of response about the 0° position gives additional confidence that the alignment was accurate.

The Čerenkov source is monitored by a smaller Hamamatsu photomultiplier, type R1635, serial number WA1781, to provide a coincidence condition for the detection of Čerenkov photons. The coincidence rate was typically 40 Hz. The housing for the apparatus is a large copper box which acts as an electromagnetic shield to attenuate radio-frequency interference. This box is surrounded by two magnetic field coils oriented to cancel the local magnetic field. The operation of these coils was verified using a flux probe in the position of the test photomultiplier. The residual magnetic field in the region of the photomultiplier was always less than $1 \mu\text{T}$. This condition required a current of 304 mA in the coils, and this current was monitored throughout the experiment.

The photomultipliers were used with the standard SNO base which distributes a fraction $\sim 8/17$ of the total applied voltage across the first stage (K - D1). The interdynode potential differences are all similar, as $1 \text{ M}\Omega$ resistors are used between each of the nine dynodes. M.H.V. cables were used, with intrinsic impedance 75Ω . A simple R-C filter was used as a signal 'pick-off' to separate the high voltage D.C. supply from the photomultiplier signals. These signals (from test and monitor photomultipliers) are then used to trigger Constant Fraction Discriminators and then Coincidence, ADC and TDC camac modules. The ADC was found to have a 'off-set' or pedestal charge, probably due to input bias current in the ADC pre-amplifier. This pedestal charge was found by opening the gate with the input terminated by a 50Ω co-axial terminator and by opening the gate with no input, resulting in a pedestal of +16 channels in both cases. Both the TDC and ADC channel sensitivity and linearity had been calibrated previously, and were found to be 0.23 ps/channel and 0.25 pC/channel respectively, with negligible non-linearity.

A scaler was used to count both coincidence rates and the 'singles' rates from the photomultipliers. The coincidence resolving time $\tau = \tau_1 + \tau_2$ was chosen to be 100 ns, so that no signals were lost to photomultiplier transit time spread (TTS), and also that reflections from the very largest signals only triggered the coincidence unit once. The discriminator level for the test photomultiplier was set to about $1/4$ of a single photoelectron signal, which was estimated from the peak of the pulse height distribution (i.e. the modal charge deposited). This discriminator level was monitored throughout the experiment using the ADC and by measuring the level-test voltage from the discriminator itself. The discriminator for the monitor photomultiplier was kept at a very small fraction (about $1/10$) of the charge deposited by a single photoelectron, which was monitored in a similar manner. With such monitoring it was possible to make a comparison (of the efficiency) between different photomultipliers, as well as different points on a single photocathode.

After a photomultiplier was installed in the apparatus and the latter made light-tight, the photomultiplier was allowed to operate at full voltage in order to reduce the noise count. This ageing is usually substantially complete after several hours. After ageing overnight, all the photomultipliers tested here had dark noise rates of less than 4 kHz. Once the normal operation of the photomultiplier had been established by the measurement of parameters such as TTS, dark noise and gain, the photocathode was scanned with the Čerenkov source. In an

over azimuthal angles.

attempt to reduce systematic error, the order of measurement of the angles was determined randomly in advance of the experiment. The pointer which adjusts the angle of the source with respect to the photomultipliers was always moved in the same direction (from negative angles to positive) to avoid backlash errors. However the apparatus did not appear to suffer from significant backlash.

The coincident noise background was continually measured during the data taking. The background was estimated by moving the source to the -90° position, at which the photocathode was not illuminated. This was used as a 'source off' position. The coincidence noise rates observed were always verified to be consistent with those predicted from the random coincidence formula, $C = n_1 n_2 \tau$, for independent noise rates n_1 and n_2 and resolving time τ . No significant cross-talk was observed. An estimate of the efficiency of the photomultiplier and discriminator to detect photons was made by taking four counts at positions OFF, ON, ON, OFF, where the ON position is the angle of interest. This order was chosen so that drift in the random noise rate of the photomultiplier cancels to first order (linear). Since the noise drifts observed were extremely small, this procedure was more than adequate. All counts referred to in this experiment were based on a 100 second time interval.

Resolution and Uncertainties

There are several sources of systematic uncertainty associated with the geometry of the source and photomultiplier arrangements. In particular, the measured efficiency as a function of position is the actual efficiency convoluted with the resolution function which describes the width of the light 'spot' on the photocathode. A black tape mask of width 18 mm was fixed to the photocathode (of photomultiplier GG3077) to estimate the width of this resolution function and to confirm that the translation between angle measured and position was consistent. The position of the tape was chosen so that one edge of the mask was near the critical angle $\theta_c \simeq 39.56^\circ$ where the radius of curvature changes from about 126 mm to about 60 mm. The other side of the tape mask lies at an angle of about 50° , in the region of particular interest for reflector design. As before, angles refer to that between the axis of the photomultiplier. The position of the black mask is shown in figure 1.

Figure 2 shows the data obtained from a scan of photomultiplier GG3077 with the black mask in place, and the lower graph in figure 2 shows an enlargement of the region near the mask. From these data the position of the source cut-off can be deduced and corresponds to that of the mask edges to within uncertainties (a couple of mm). The principal limitation being the measurement of the position of the mask in relation to the meridian of the photomultiplier. The width of the resolution function can be determined crudely from the slope of the intensity/angle at the edge of the mask. Hence we may deduce that the full width at half maximum of the resolution function is about 2 mm at 42° and about 4 mm at 50° . As expected the width of the resolution function increases at large angles (greater than θ_c) as the source moves off the surface of the photomultiplier. It is likely that the width of the resolution function will increase in the region up to the aluminised layer. The width could be as wide as 7 or 8 mm.

Random fluctuations influence both the accuracy to which the angle pointer can be adjusted and read, and also the number of counts observed at each angle. An estimate of the setting accuracy of the source position can be deduced from the steep fall of count rate with angle at 42° with the black mask in place. The total setting accuracy is consistent with a standard deviation of about 0.5° or about 1 mm along the surface of the photomultiplier. Since the signals recorded are always the result of coincidence from two photomultiplier's it is thought that Poisson statistics will provide a good estimate of the error of the total observed count rate. On this basis, the typical standard error would be of order of 50 counts

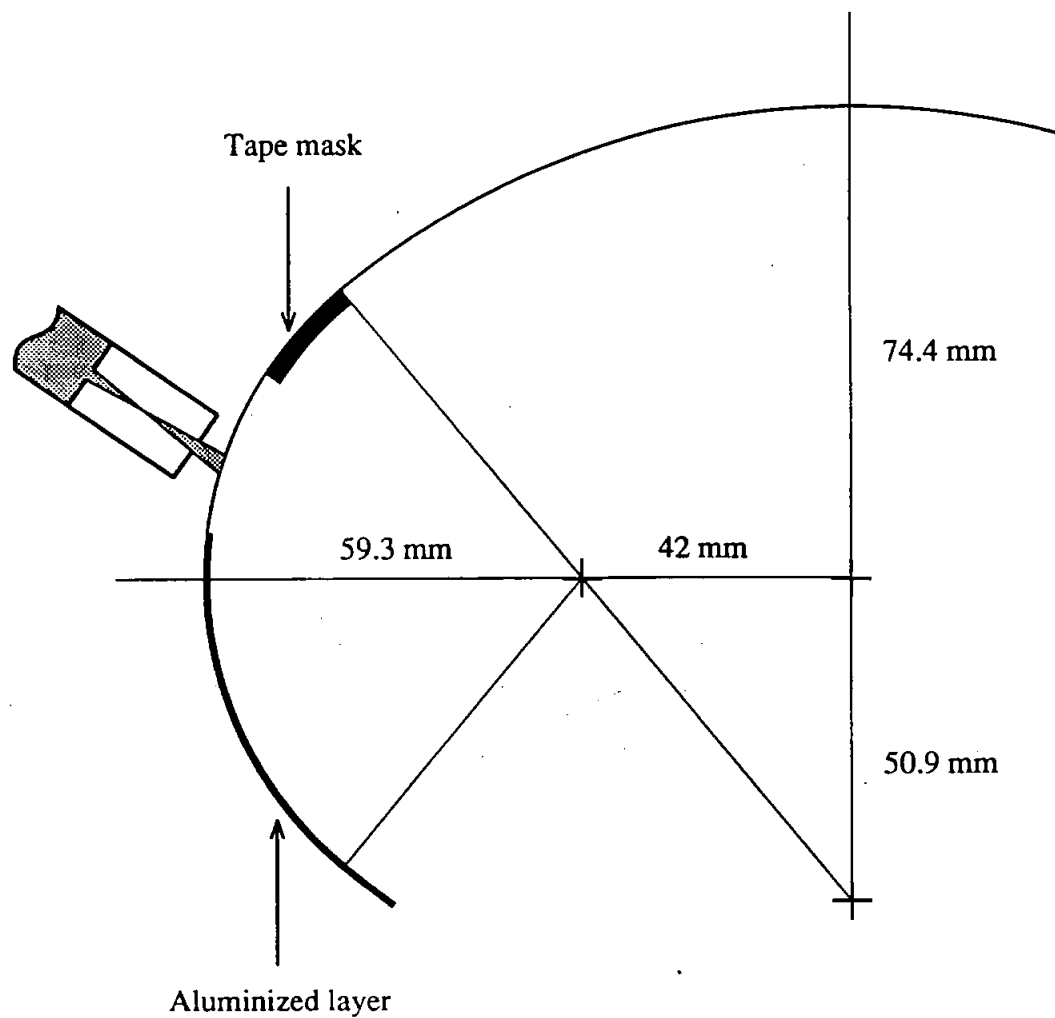
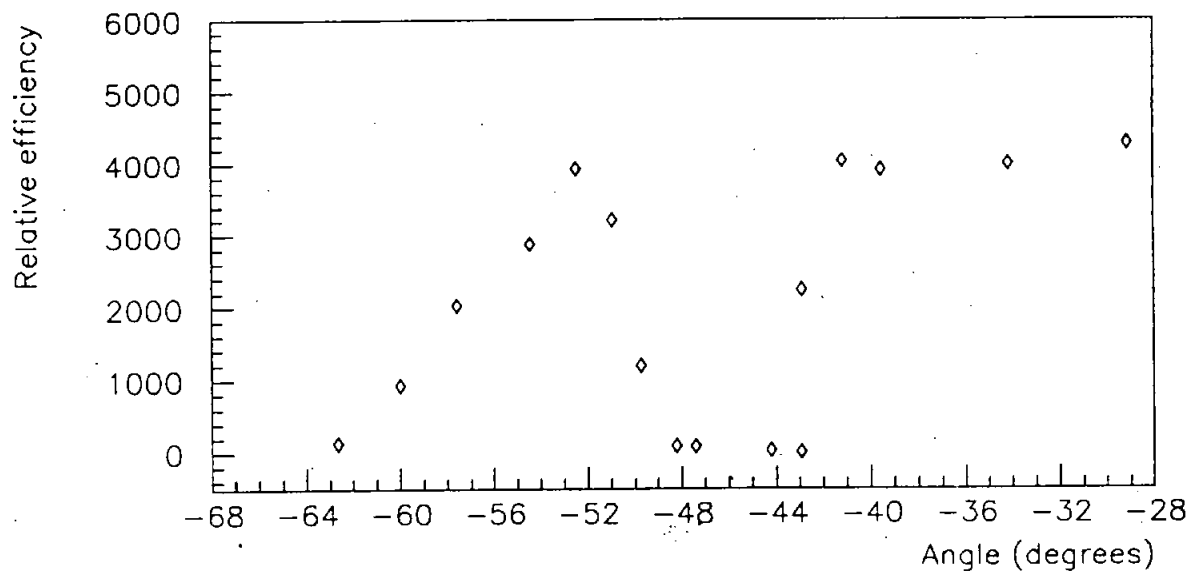
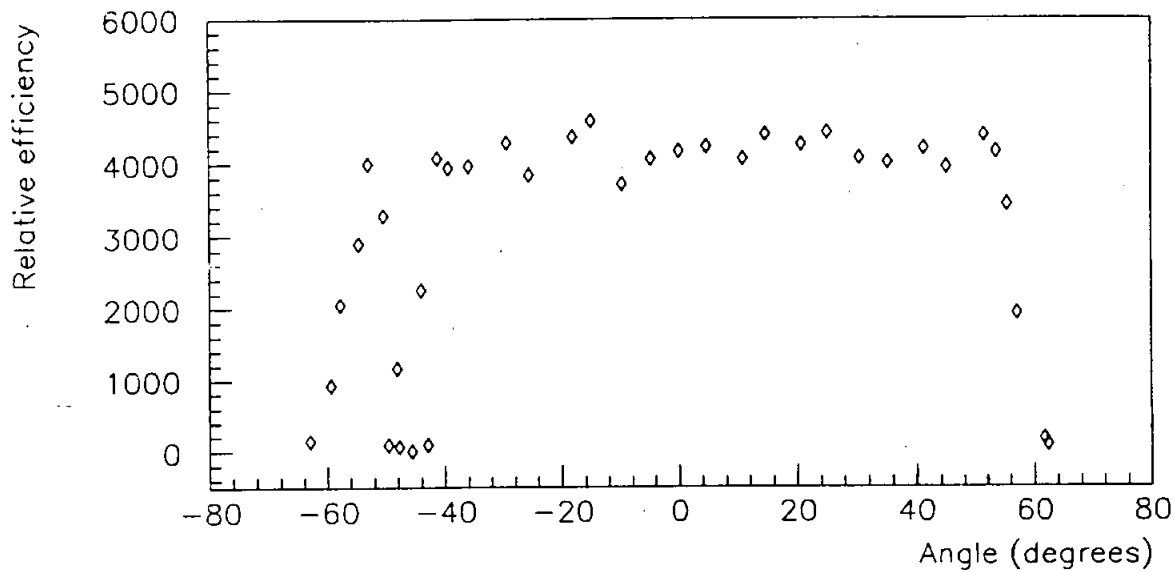


Figure 1: Shape of the Hamamatsu R1408 photomultiplier bulb. The approximate position of the black mask used on photomultiplier GG3077 is shown. The dimensions are those deduced from measurements of the bulb shape.



GG3077

Figure 2: Photocathode scan of GG3077. The interval $-50^\circ \rightarrow -42^\circ$ was masked with black tape and the lower graph shows the data in this region. The positional accuracy is good at the level of 2 mm, and the resolution is 2 mm at 42° and 4 mm at 50° .

Start time	Reading number	Net counts in 100 s
11:19 am	8	2719
12:32 pm	16	2768
12:58 pm	19	2889
3:34 pm	35	2820
4:02 pm	38	2852
Estimate of Mean \bar{x}		2809.6
$\sigma_{n-1}(x_i)$		60.25
$\sigma_{n-1}(\bar{x})$		30.13

Table 1: Random fluctuations of scan measurements.

in 100 seconds. A test was devised which would estimate this standard error with the typical contribution from the error due to angle setting. During the course of measurements of photomultiplier CB0265, five independent measurements of the count rate at an angle of -55° were taken. The count rate is changing relatively quickly with position in this region, so that angular setting errors would also influence the observed spread of values. These five measurements were taken using similar procedure as other points, interleaving them with the normal pattern of points at random intervals. The results are shown in Table 1.

The parameter $\sigma_{n-1}(x_i)$ shows an unbiased estimate of the standard deviation of the single measurement (population) distribution, whereas the parameter $\sigma_{n-1}(\bar{x})$ shows an unbiased estimate of the standard deviation of the mean estimator \bar{x} . The single measurement error $\sigma_{n-1}(x_i)$ of about 60 counts in 100 seconds is consistent with the estimated value of 50 counts in 100 seconds.

Scan results

Before each photomultiplier was scanned using the source, the operating parameters were measured to ensure the tube was operating correctly. With the source spot at 0° , the spot scan parameters were recorded, and these are shown in Table 2.

Column 3 of the table shows the total voltage applied to the photomultiplier in order to achieve a gain of 10^7 , but note that an additional voltage is dropped across the resistor in the signal pick-off circuit which makes the required power supply voltage greater than the figures quoted in the table. Column 4 shows the full width at half maximum of the transit time spread distribution in nanoseconds, for a spot illumination. Note that the transit time spread times recorded here are smaller than those for total illumination of the photomultiplier front window. The right hand column shows the dark noise rate in kHz after about 16 hours of operation in the dark. It is likely that the noise rate would subsequently decrease further.

Figure 3 show the results of the photocathode scan for these Hamamatsu R1408 photomultipliers with SNO bases. The errors on each point are approximately 60 counts in 100 seconds. It is clear that there are local variations of photocathode sensitivity which are statistically significant. However, it is likely that their nature is random and that the average

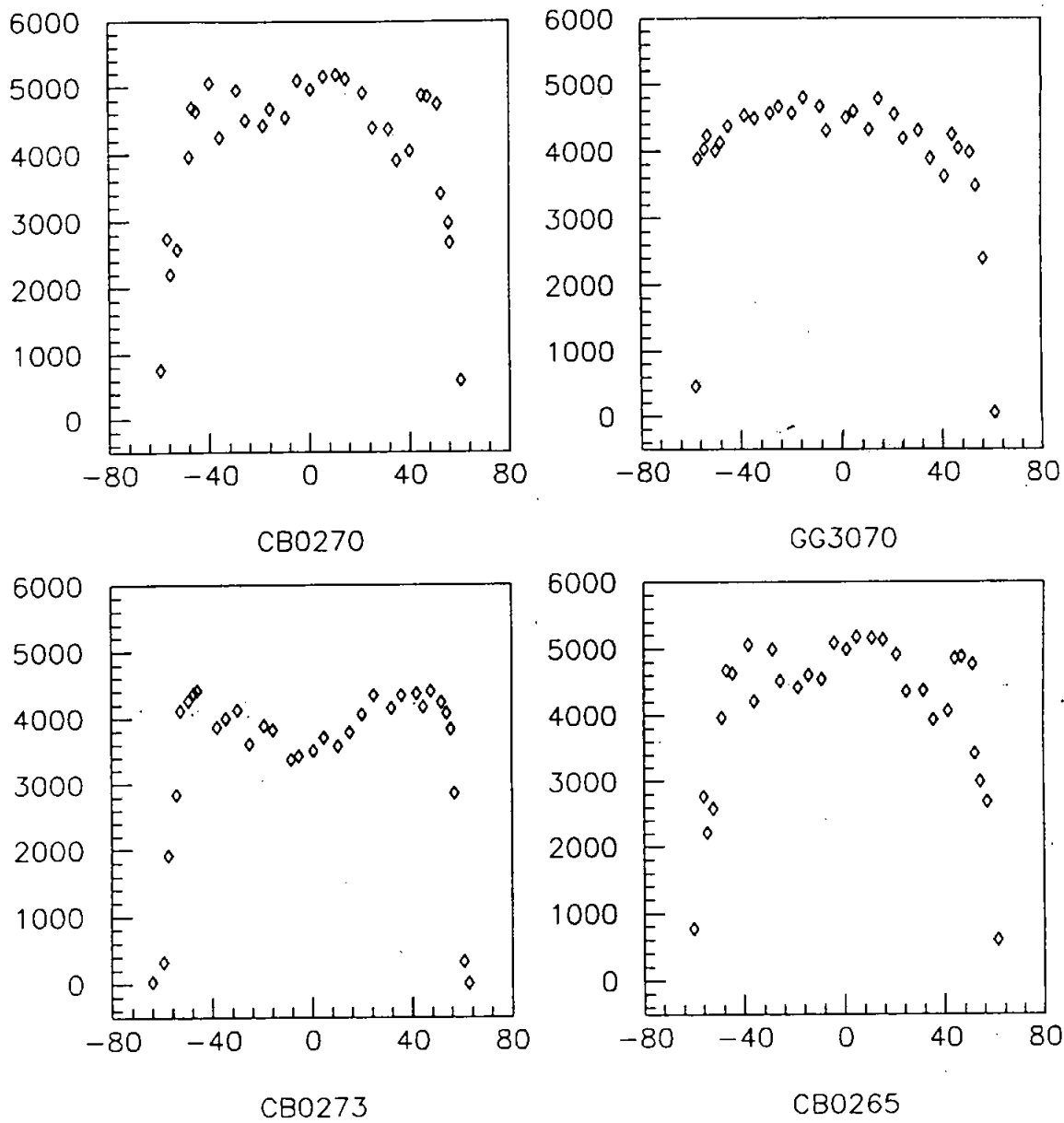


Figure 3: The results of the photocathode scans as a function of angle. The relative efficiency is shown on the ordinate axis expressed in terms of the number of counts observed in 100 seconds. The standard deviation of this figure is about 60 counts in 100 seconds.

Experiment date	Serial number	Total volts	TTS (ns)	Noise (kHz)
27 th September	CB0270	1700	N/A	3.0
1 st October	GG3070	1830	3.04	1.2
2 nd October	CB0273	2370	3.11	1.2
3 rd October	GG3077	2120	3.04	2.5
4 th October	CB0265	2270	2.80	4.0

Table 2: Photomultiplier spot scan parameters.

photomultiplier response will be flat in the region inside the boundary of the photocathode. The determination of the position of the photocathode boundary will be considered further in the next section.

The radial extent of the photocathode has implications for the maximum lower diameter of the reflectors to be used on the SNO photomultipliers. For this reason it is required that the measurements of angle be converted to effective radius from the axis of the photomultiplier, and this in turn requires accurate knowledge of the photomultiplier bulb shape ². The bulb is made with radius of curvature of 126 mm for $\theta < \theta_c$ and 60 mm for $\theta > \theta_c$, where $\tan \theta_c = a/c$, see Table 3. The centre of the smaller circle is given as 42 mm. The bulb is the resulting surface of revolution.

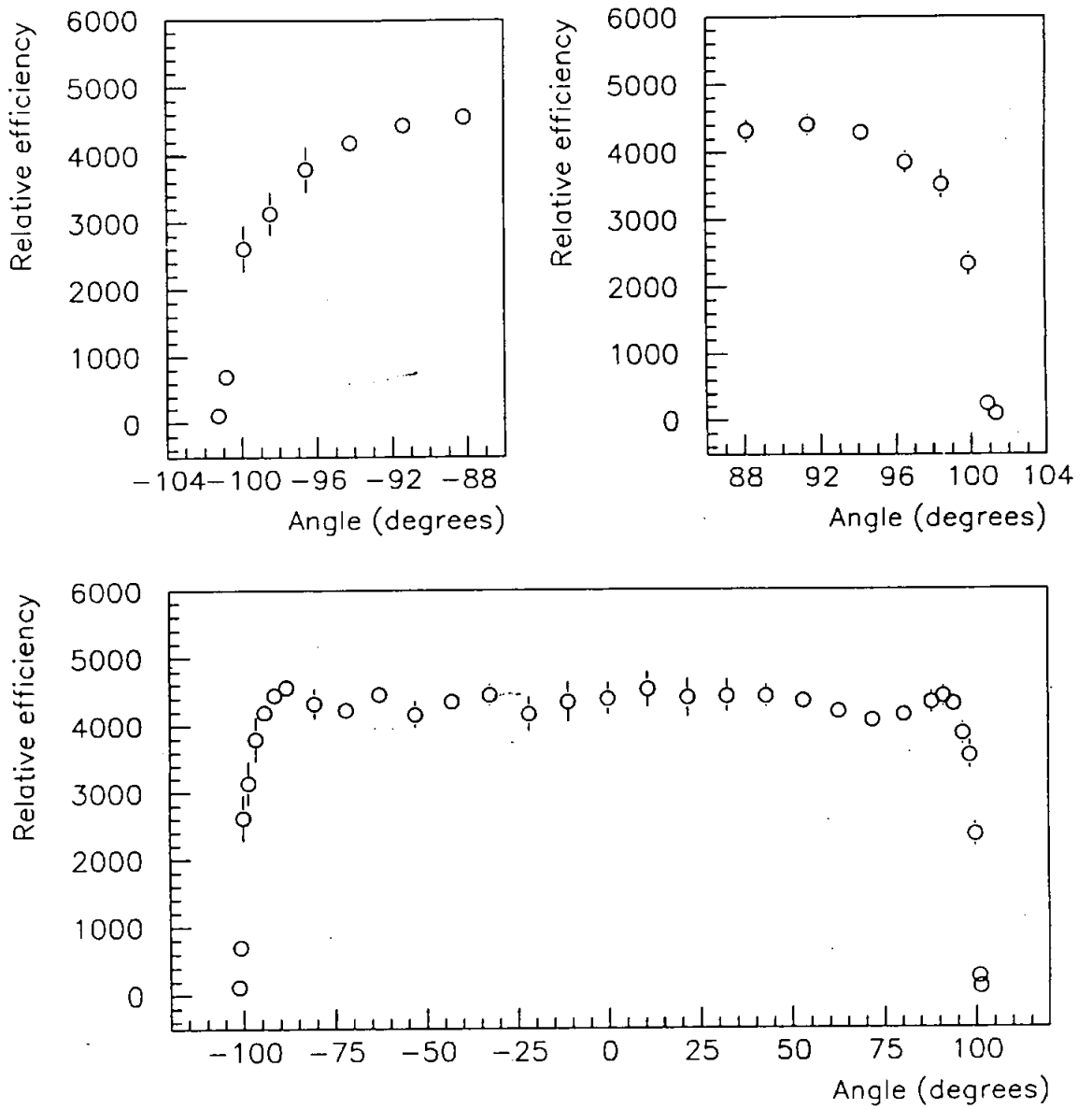
The assumed values are shown in Table 3. Using these assumed values the radius $r(\theta)$ may be deduced from the measured angle as follows: For $\theta < \theta_c$ the radius is simply given by $r(\theta) = (c + d) \sin \theta$. For larger angles the radius is given by

$$r(\theta) = \frac{(a + c \cot \theta) + [(a + c \cot \theta)^2 - (1 + \cot^2 \theta)(a^2 - b^2 + c^2)]^{1/2}}{1 + \cot^2 \theta} \quad (1)$$

Using this relation it is possible compute the radii as a function of theta for the angles measured. In order to assess the data from all five photocathode scans, these data sets have been averaged and the results plotted as a function of radial distance from the photomultiplier axis. These data are shown in figure 4. The error bars on the points are estimators of the unbiased standard deviation of the mean number of counts measured in 100 seconds. Of course the single photomultiplier distribution will vary by an amount $\sqrt{5}$ larger than the displayed error bars. Near the edges of the photomultiplier the count rate falls rapidly with increasing radius, so enlargements of these regions are shown in figure 4 for negative and positive radii.

These figures clearly show that the photocathode extends almost all the way to the photomultiplier equator. The data are consistent with a photocathode which is quite uniform on average, but has local deviations from this average. It should be noted that the resolution function will smear this function by an amount of about 8 mm divided by the tangent of the angle of the normal with respect to the photomultiplier axis, at each point. Near the edge (say $r = 100$ mm) this resolution width is only about 1.5 mm in axial radius. With this in mind, an assessment of the impact of the photocathode response has now been made, and a

²The photomultiplier bulbs are made by Schott subject to drawing number A5349-00-02d, which is supposed to describe the shape of the bulb.



Average efficiency for 5 photomultipliers

Figure 4: The lower plot shows the average of the photocathode scans as a function of radius. Positive radii correspond to positive angles. The relative efficiency is shown on the ordinate axis. The upper plots show enlargements of the edge regions.

Shape parameter	Schott value (mm)	Assumed value(mm)	Label
Radius of curvature ($\theta < \theta_c$)	126	125.3	$c + d$
Radius of curvature ($\theta > \theta_c$)	60	59.3	b
Top of photocathode to equator along the PMT axis	75.1	74.4	d
Distance from PMT axis to centre of curvature for $\theta > \theta_c$	42	42	a

Table 3: Hamamatsu R1408 bulb shape parameters.

decision has been made by the SNO reflector committee to use an area of the photocathode of radius 98 mm.